

Space Domain Reflectometry for opens detection location in microbumps

J. Gaudestad^{a,*}, V. Talanov^a, P.C. Huang^b

^a Neocera, LLC, 10000 Virginia Manor Road, Beltsville, MD 20705, USA

^b TSMC, Hsinchu Science Park, Hsinchu 300-77, Taiwan, ROC

ARTICLE INFO

Article history:

Received 2 June 2012

Received in revised form 9 July 2012

Accepted 10 July 2012

Available online 15 August 2012

ABSTRACT

Space Domain Reflectometry is a newly developed non-destructive failure analysis technique for localizing open defects by imaging the magnetic field generated by a radio frequency (RF) current induced in the sample. The technique was used to locate a cracked microbump in a daisy chain between two full 725- μm -thick dies.

© 2012 Elsevier Ltd. All rights reserved.

1. Introduction

Short and open issues are common in back-end-of-line process (BEOL) in a wafer foundry as well as in package manufacturing, especially as integrated circuit (IC) devices become smaller and devices are stacked in a 3D formation. This is induced by modifications in the process flow such as application of low-k dielectric material, thinner inter-metal-dielectric layer and lithography issues as well as using new package and substrate material that is flexible [1]. In the past, most failure analysis tool makers have been focusing on solving short and leakage failures using techniques such as liquid crystal analysis (LCA), laser scanning microscopy (LSM), infrared thermal detection (ITD) method and focused ion beam (FIB) circuit edit (CE) and Magnetic Current Imaging (MCI) [2].

1.1. Time domain reflectometry

While the above techniques are capable of visualizing the current shorts and leakages in the packages or input/output-stages of dies, there has only been Time Domain Reflectometry (TDR) to localize opens electrically. TDR uses a pulse generator and a high-speed oscilloscope to record in real time the reflection of a microwave signal by the open barrier [3,4]. TDR can at best provide resolution of about 1 mm making it most suitable for the high-pin-count packages, such as quad flat package and ball grid array, but less convenient for smaller packages (less than 1 cm²) [5], and more or less impossible to use on the latest development for connecting dies in wafer leveling packaging using microbumps. An extension of the TDR technique employs a Vector Network Analyzer (VNA) to obtain the device response in the frequency domain by applying a continuous wave and then measuring the reflected wave. The time domain signal can then be calculated by inverse

Fourier-Transformation of the frequency domain data. The effect of improved detail resolution with increasing bandwidth is well known and the bandwidth can be as high as 110 GHz for a VNA [4].

1.2. Magnetic current imaging

Magnetic Current Imaging (MCI) has for years been used to detect shorts and leakages in packages and dies. The technique utilizes two types of sensors: Superconducting Quantum Interference Device (SQUID) sensor for low current and large working distances and a Giant Magneto Resistor (GMR) sensor for sub micron resolution current imaging at wafer/die level. Both sensors have been working at frequencies less than 100 kHz due to the constraints of the electronics and sensor wiring [6].

MCI imaging of packaged devices is accomplished using a high-critical-temperature ($T_c = 90$ K) SQUID to measure the vertical (\vec{Z}) component of the magnetic fields surrounding conductors carrying current to, from, and through short circuits. An AC bias is utilized on the sample to enable lock-in amplification for noise reduction [7]. Magnetic field data are transformed into current density images [8] which typically show higher gradients inherent in localized narrow current paths or dissolution of current density where narrower paths dissipate to much broader conductors or power planes at short circuit sites. Current direction is also easily determined as the fields surrounding active conductors are bipolar [9].

In this paper, we show that by increasing the bandwidth of the SQUID electronics, MCI can image open defects in microbumps through full thickness die of 725 μm using a two dimensional image, basically taking magnetic field data in the space domain giving the name to the newly developed technique Space Domain Reflectometry (SDR).

2. Principle of open detection using magnetic fields

DC and low frequency signals, normally used in electrical probing of ICs, cannot carry current through the open trace because of

* Corresponding author.

E-mail address: gaudestad@neocera.com (J. Gaudestad).

its high impedance. If the signal frequency is brought into the radio-frequency (RF) range, the defective trace can be viewed, likewise to TDR, as an open-circuited transmission line. By modeling the open, either physical or electrical, as a parallel connection of resistance R and capacitance C we obtain for its impedance:

$$Z_{open} = \frac{R}{1 + (\omega RC)^2} + i \frac{\omega R^2 C}{1 + (\omega RC)^2} \quad (1)$$

where $\omega = 2\pi f$ is the angular frequency of RF probing signal. Depending on the ωRC product value, Z_{open} may be predominantly resistive or capacitive. For instance, at 100 MHz the representative $R = 1 \text{ M}\Omega$ and $C = 1 \text{ fF}$ yield $\omega RC \sim 1$, making $|Z_{open}|$ in $\text{M}\Omega$ range.

The SDR technique injects RF signal ranging from 60 to 200 MHz into defective trace via feed-line formed by RF probe. Modeling the trace as a transmission line of characteristic impedance Z_0 ($\sim 50 \Omega$) terminated by Z_{open} , we obtain for the reflection coefficient of the probing RF signal:

$$\Gamma = \frac{Z_{open} - Z_0}{Z_{open} + Z_0} \approx 1 - \frac{2Z_0}{Z_{open}} \approx 1 \quad (2)$$

where the expansion is due to $Z_0 \ll Z_{open}$. This condition causes the open to reflect all the incident RF power back toward the feed-line. A superposition of the incident and reflected waves forms a standing wave [10] in the trace, in which the current node coincides with the open location. Fig. 1 schematically shows variation of the standing wave current amplitude along the open-circuited trace.

Since for typical ICs at RF frequencies $z \ll \lambda$, one can make the approximation that the current linearly decays in vicinity of the open due to $\sin(\beta z) \approx \beta z$. The amplitude of a standing wave current varies versus position along the trace as:

$$I = 2\sqrt{\frac{P}{Z_0}} \sin(\beta z) \approx 2\sqrt{\frac{P}{Z_0}} \beta z \quad (3a)$$

where P is the incident RF power, $\beta = 2\pi/\lambda$ is the wavenumber of a probing signal with λ the wavelength, and z is the position along the trace with the open located at $z = 0$.

Substitution of $\beta = 2\pi/\lambda$ and $\lambda = c/f$ into Eq. (3a) yields:

$$I = 4\pi\sqrt{\frac{2P}{Z_0}} \cdot \frac{z}{\lambda} = \frac{4\pi}{c} \sqrt{\frac{P}{Z_0}} \cdot fz \quad (3b)$$

where c is the speed of RF signal propagation in transmission line formed by the trace. Merging the constants $(4\pi)/(c\sqrt{Z_0})$ yields the following relationship between the RF current (I), power (P), frequency (f) and distance from the open location (z):

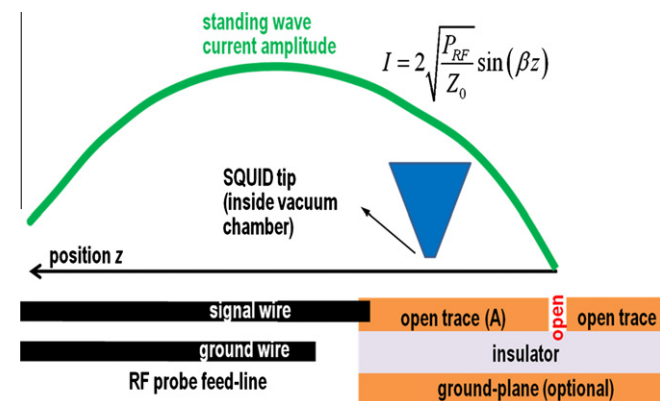


Fig. 1. Cartoon of a half-period of the standing wave formed in the open-circuited trace. The feed-line signal wire is ohmically connected to the defective trace, and the ground wire may be either left floating (shown) or connected to the IC ground-plane.

$$I \propto \sqrt{P} \cdot f \cdot z \quad (3c)$$

Since the open is located at $z = 0$ the current will always be zero at the open location. Inspection of Eq. (3c) shows that in order to improve the open localization accuracy, both the RF power and frequency must be as high as practical, to cause a “steeper” decay of detected RF signal closer to the open location.

Scanning SQUID RF Microscope “Magma” images the magnetic field of a standing wave in vicinity of the open, which allows recovering the standing wave current profile and locating the open. Unlike TDR, SDR’s spatial resolution is not limited by the frequency but rather the SQUID size and sensor-to-trace distance, enabling it to locate opens in the package as well as in silicon with accuracy below $30 \mu\text{m}$.

3. Sample: double stacked microbumps

As Wafer Level Packaging (WLP) is becoming more common as a procedure to connect dies in a 3D formation, the drive to shrink the footprint has led to the development of microbumps that are considerably smaller than the C4 solder bumps used for connecting a flip chip die to the substrate. When the die size increases, the number of failures and failure modes in the microbumps also increases. Cracks and open failures in the microbumps have been a challenge to find non-destructively, with X-ray having been the only viable option. With the shrinking size of the individual microbumps and the increasing number of microbumps (in the thousands) proportional to the increasing size of the dies, it has become very time consuming to use XRay inspection at high resolution to find the open microbump.

The double stacked die being tested in this Fault Isolation consisted of one full thickness ($725 \mu\text{m}$) silicon die with three smaller full thickness ($725 \mu\text{m}$) dies on top (see Fig. 2). The bottom die is $26 \times 24 \text{ mm}$ in size, while the top three dies form a rectangular shape of $24 \times 22 \text{ mm}$ in size, exposing the 2-mm-wide edge of the bottom die for probing, where the test pads of $40 \times 60 \mu\text{m}$ in size enable for electrical connections to the daisy chains. Top Die 1 measures $24 \times 15 \text{ mm}$ while Top Dies 2 and 3 measure $12 \times 7 \text{ mm}$ each. The C4 bumps have diameter of $200 \mu\text{m}$ and the microbumps have a diameter of $45 \mu\text{m}$.

The two dies are connected using microbumps in a sandwich-like buildup with the metal layers in between the two dies in the stack (Fig. 3). The dies have no active components.

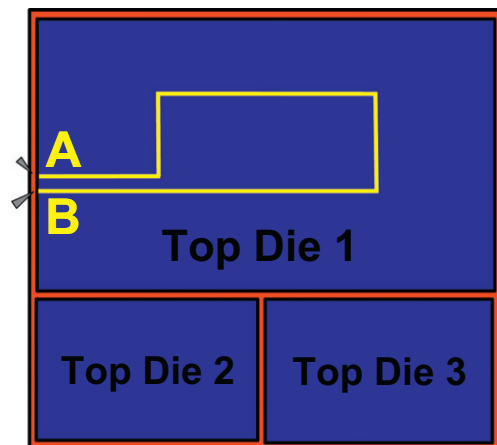


Fig. 2. Top view of the double stacked die. The bottom die (red) has three dies on top (blue). The Top Die 1 has a daisy chain (yellow path) with a cracked microbump. The RF probes are connected to the bottom die.



Fig. 3. Side view of the double stacked die connected using microbumps in a daisy chain structure with a cracked bump showing open on electrical test measurement.

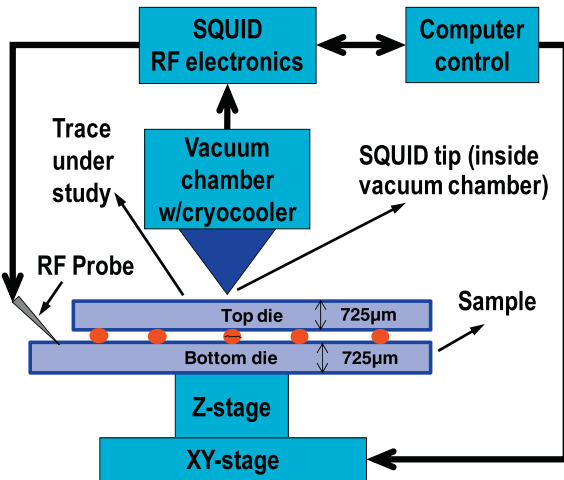


Fig. 4. The SQUID is under vacuum while the sample is at room temperature on top of an XY stage. RF Probers inject the RF signal onto the sample under test.

4. Experimental setup

Electrical testing showed that the defective double stacked die sample had 720 kΩ resistance between probe point A and probe point B (yellow¹ path in Fig. 2) while a good comparable sample had 3 kΩ resistance between the same probe points. This higher resistance indicated a cracked microbump or metal trace crack, rather than a fully open which would have shown a resistance in the tens of megaohms. Since TDR is not a viable option for opens detection in silicon, SDR was the only technique for non-destructively locating this opens defect. The signal can be injected from either test point A, test point B, or both test points A and B at the same time (see Fig. 2).

A newly developed Magma Electric Fault Isolation (EFI) system with high frequency electronics was used for imaging the RF signal induced in the open trace (Fig. 4).

MCI was achieved using high frequency electronics for pumping a signal into the sample under test and to run the SQUID and the SQUID electronics at 60 MHz. RF probers were used to inject the RF signal into the daisy chain structure (Fig. 5).

5. Magnetic current imaging results

The current images acquired with the 60 MHz RF signal are shown in Fig. 6a–c overlaid the optical images for reference.

Fig. 6a–c shows the RF current when injecting the signal from either one test point at a time (Fig. 6a and b) and letting the other test point floating (it does not need to be grounded), or sending in a signal at both test points simultaneously (Fig. 6c). One can clearly see that all three data sets are pointing out to the same location (red arrow) for the open failure where the RF current decays to zero level.

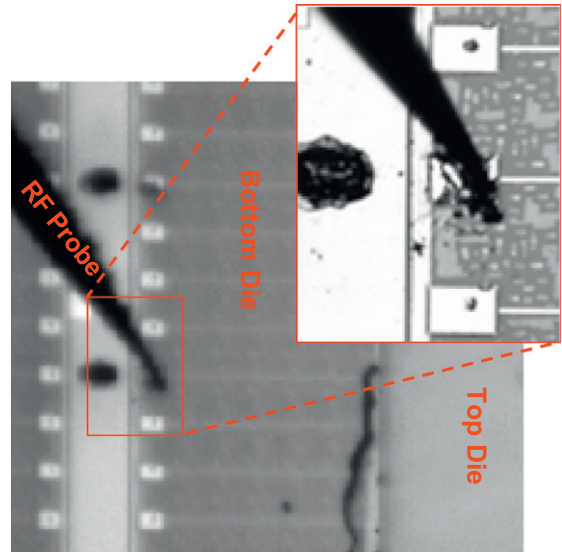


Fig. 5. Showing the probe needle making electrical connection to probe point B.

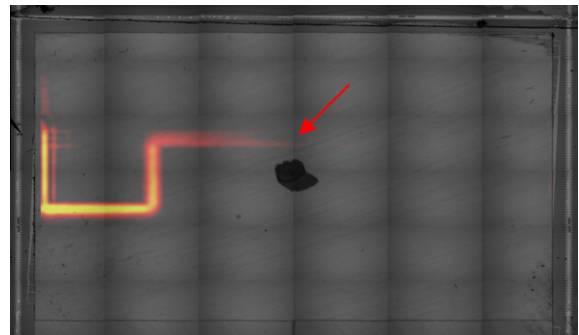


Fig. 6a. Probe point A having RF signal showing reflection at open location.

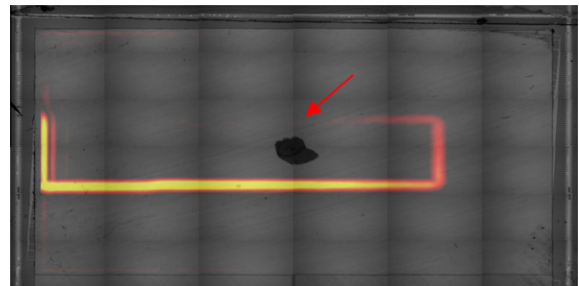


Fig. 6b. Probe point B having RF signal showing reflection at open location.

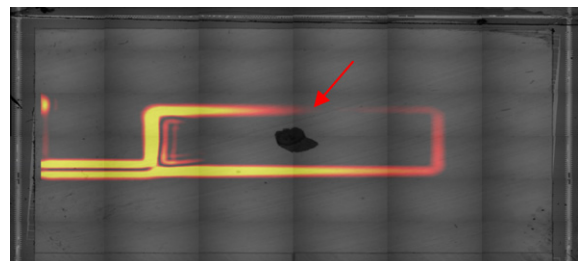


Fig. 6c. Probe point A and B having RF signal injected at the same time, showing signal reflecting at the same location.

¹ For interpretation of color in Figs. 1–8, the reader is referred to the web version of this article.

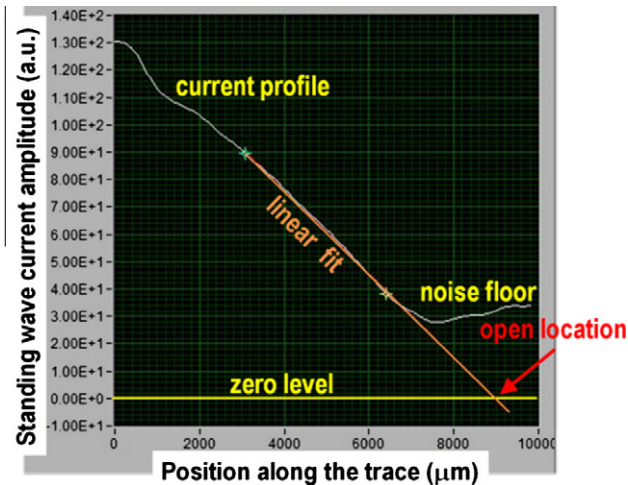


Fig. 7a. Shows the linear decay of the signal. Open location is where the signal amplitude extrapolates to zero.

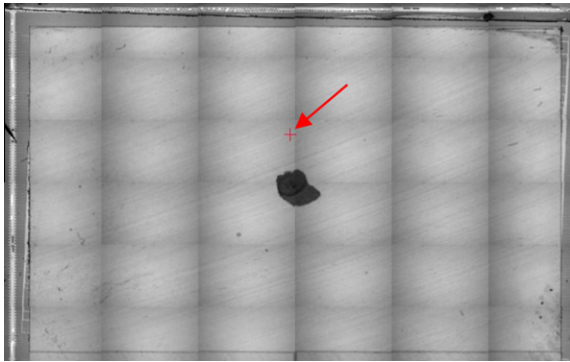


Fig. 7b. The software automatically puts a crosshair in the optical image where the open location was found using the linear decay model.

5.1. Linear decay analysis

In order to accurately pinpoint the open location, the following advanced data analysis technique was used. According to Eq. (3c), RF current decays linearly toward the open. In practice, however, the inevitable noise floor of the SQUID sensor prevents one from imaging RF current all the way down to the open location. By linearly fitting the current profile in vicinity of the open and extrapolating the fit toward zero level, as shown in Fig. 7a and b, the FA engineer is able to recover the open location.

Once the open physical location has been found using Magma SDR, 2D X-Ray had become a very fast way of confirming the failure location as shown in Fig. 8. The open was due to that two microbumps had been separated, causing poor connection.

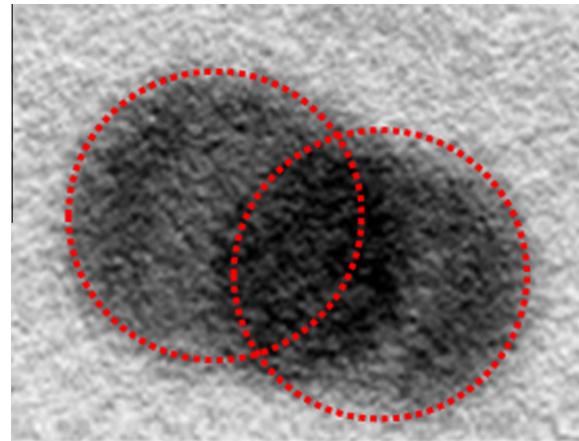


Fig. 8. The failed microbump with high resistance causing poor connection seen from 2D X-Ray.

6. Conclusions

We showed in this paper that it is possible to use Magnetic Field Imaging technique with a high frequency SQUID using Space Domain Reflectometry to image the location of a dead open. Current results are showing a resolution of around 30 μm but further data analysis improvement shows that one can find the open to within 10 μm accuracy.

References

- [1] Tan PK, Mai ZH, Toh SL, Hendarto E, Deng Q, Goh YW, et al. Chartered semiconductor manufacturing Pte. Ltd. Physical failure analysis techniques and studies on vertical short issue of 65 nm devices. In: ISTFA 2008 proceedings.
- [2] Len WB, Liu YY, Pang JCH, Chan DSH. Near IR continuous wavelength spectroscopy of photon emissions from semiconductor devices. In: ISTFA 2003 proceedings, p. 311–16.
- [3] Dong-Ho Han, Bao-Shu Xu, Myoung J. Choi, Jiangqi He, Scott Gardiner, Cliff Lee. Intel Corporation. Realization of ultra-wideband high-resolution TDR for chip-carrier packages. ASME InterPak San Francisco 2005.
- [4] Krueger B, Pohl H, Schumann F, Schoemann S. Infineon Technologies AG, Munich, Germany. Advanced localization technique of failures in packages/IO-stages of chips using vector network analyser. In: IPFA 2008 proceedings.
- [5] Abessolo-Bidzo D, et al. Isolating failing sites in IC packages using Time Domain Reflectometry: case studies. In: Proc. 15th Eur. symp. reliab. electron devices (ESREF); 2005.
- [6] Crepel O, Poirer P, Descamps P. LaMIP Philips Semiconductor. Magnetic microscope for ICs failure analysis: comparative case studies using SQUID, GMR and MTJ systems. In: IPFA proceedings 2004.
- [7] Hsiung SK, Tan KV, Komrowski AJ, Sullivan DJD. LSI logic, failure analysis on resistive opens with scanning SQUID microscopy. In: IRPS 2004.
- [8] Roth BJ, Sepulveda NG, Wikswo JP. Vanderbilt university, using a magnetometer to image two-dimensional current distribution. J Appl Phys 1989;65(1):361.
- [9] David P. Vallett. IBM Systems & Technology Group, Essex Junction, VT, USA. A comparison of lock-in thermography and magnetic current imaging for localizing buried short-circuits. In: ISTFA proceedings 2011.
- [10] Pozar D. Microwave engineering. J. Wiley; 2005.